Journal of The Electrochemical Society, **153** (9) A1672-A1677 (2006)
0013-4651/2006/153(9)/A1672/6/$20.00 © The Electrochemical Society

Model of a Direct Methanol Fuel Cell Stack

Resistive "Spots" and Stack Performance

A. A. Kulikovsky[*,z]

Institute for Materials and Processes in Energy Systems (IWV–3), Research Center "Jülich," D–52425 Jülich, Germany

We report on a model of a direct methanol fuel cell stack. The model is based on our recent model of a single cell with parallel straight channels. The stack model accounts for voltage loss due to in-plane currents in the bipolar plates and local "spots" of contact resistance. A 100 cell stack with a various number of spots is simulated. The effect of spots is twofold: they (*i*) increase local current and polarization voltages in the unaffected part of the cells, and (*ii*) induce in–plane parasitic current in bipolar plates. The growth of local current in the unaffected part of the cells reduces limiting current density of the stack. The stronger stack contamination with the spots, the lower the limiting current density. In the studied range of parameters, voltage loss in the bipolar plates is negligible.
© 2006 The Electrochemical Society. [DOI: 10.1149/1.2213460] All rights reserved.

Manuscript submitted December 19, 2005; revised manuscript received March 14, 2006. Available electronically June 30, 2006.

In recent years direct methanol fuel cells (DMFCs) have attracted much attention in academic institutions and companies. The advantage of a liquid fuel makes DMFC a viable candidate for replacement of Li–ion batteries in mobile applications.

The major problems in DMFCs are sluggish kinetics of methanol oxidation and methanol crossover from the anode to the cathode side.[1] CO_2 bubbles in the anode channel may also seriously decrease DMFC performance.[2-4]

To achieve high volumetric power density, the cells are assembled in a stack, which typically consists of 10–100 cells. This leads to another overhead: transport of current through the stack induces voltage losses in bipolar plates (BPs), which interconnect individual cells. Qualitatively, when the distribution of local current over the surface of adjacent cells is essentially different, a significant fraction of current is transported along BPs and wastes electric power.[5]

Another problem in DMFC stacks is numerous spots of local resistance, which arise due to noneven distribution of clamping pressure, local corrosion, etc. The spots increase the amount of current transported along the bipolar plates and enlarge the anode and the cathode polarization voltages in the "contaminated" cells (see below).

Buttin et al.[6] developed a 5 cell DMFC stack with the stainless steel BPs. They compared the performance of the first and fifth cells in the stack with the performance of the single cell equipped with the graphite current collectors. Both cells in the stack exhibited significantly lower performance than the stand–alone cell. This result was attributed to the effect of contact resistance in the stack, though no detailed analysis was reported.

So far modeling studies were focused on the simulation of individual cells.[3,7-12]. To our knowledge, in the literature there are no models of DMFC stacks. In this work we develop a model of a stack, which enables us to study the effects of stack contamination by the spots of high contact resistance and to calculate voltage loss due to in–plane current in the BPs.

The structure of the work is as follows. First, we present the general description of the model of a single cell with equipotential electrodes.[12,13] Then we show how to take into account voltage variation along the BPs. Local currents in the adjacent cells determine potential distribution along the BP, which interconnects these cells. Local potential difference between two neighboring BPs in turn determines local voltage of the cell between them. The stack model is thus formulated as a selfconsistent problem of voltage and current distribution in the cells and BPs. Finally, we study the effect of resistive spots on stack performance.

* Electrochemical Society Active Member.
z E-mail: A.Kulikovsky@fz-juelich.de

Model of an Individual Cell in a Stack

General description.— Individual cells in a stack are described within the scope of the model.[12,13] The idea which stands behind the model equations is as follows.

Consider DMFC equipped on both sides with the single straight channels (Fig. 1). The inlets of oxygen and methanol channels are located at $z = 0$ (coflow conditions, Fig. 1). The distribution of reactants, potentials, and currents in the plane shown in Fig. 1 is a solution to the respective 2D problem.

Analysis of governing equations shows that in the membrane electrode assembly (MEA) z–components of all fluxes are small as compared to their x–components (Fig. 1).[8] This enables us to split the 2D problem in Fig. 1 into a local 1D problem along the x–axis in the MEA and a 1D problem of the flow along the z–axis in the channels.[12,13] Following commonly accepted terminology, this is a 1D + 1D approach.

The model[12,13] takes into account diffusion of reactants across the cell (including methanol crossover) and their convective transport along the channel. The rates of electrochemical reactions on both sides of the cell are assumed to obey the Tafel law. The model[12,13] is developed for ideally conductive (equipotential) current collector plates. The equations which describe voltage loss due to in-plane current in bipolar plates are derived in Ref. 5. The approach described there is used here to take into account variation of potential along the BPs. The respective changes to the model are described in the next section.

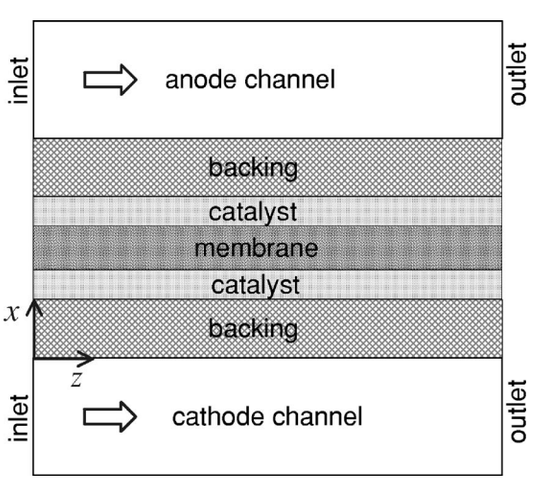

Figure 1. Sketch of the individual cell.

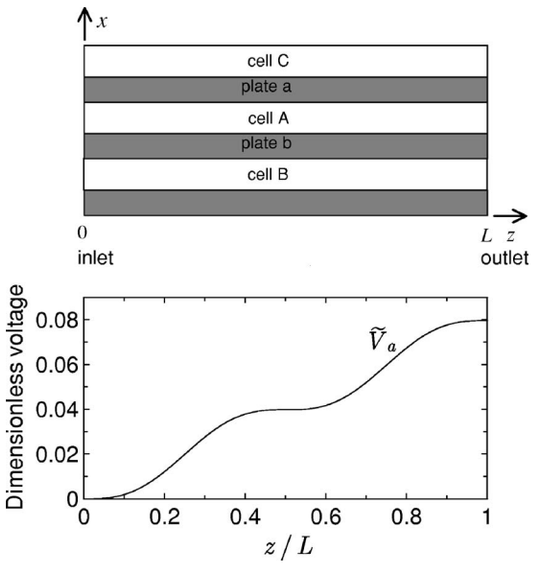

Figure 2. (top) Stack fragment. (bottom) Voltage distribution along the bipolar plate a. Note that $\widetilde{V}_a$ is calculated with respect to plate voltage at $z = 0$; potentials of the other plates are also calculated with respect to their potentials at $z = 0$.

Local cell potential.— Consider the fragment of a stack (Fig. 2). Individual cells (MEAs) are denoted by capital letters (A, B, C); the bipolar plates are marked with the small letters (a, b). We ignore the details of BP structure (channel/rib) and assume that each BP is a thin parallelepiped with isotropic conductivity.

The variation of potential across the BP (along the x–axis, Fig. 2) can be ignored, because the thickness of BP ($\simeq$0.1 cm) is typically 3 orders of magnitude lower than its length L ($\simeq$10 cm). Furthermore, we assume that BP width w along the axis perpendicular to the plane of Fig. 2 is much smaller than L; this makes it possible to ignore the respective variation of potential. Each cell in our stack is clamped between two 1D BPs (Fig. 2); BP potential V is thus a function of z only.

Variation of V along z occurs due to in–plane current in the plate. The reference point for $V(z)$ is plate potential at $z = 0$. Local voltage drop V_{ab} between the plates a and b is then

$$V_{ab} = V_0 + V_a(z) - V_b(z) \qquad [1]$$

where $V_0 \equiv V_{ab}(0)$ is voltage drop between a and b at $z = 0$ and $V_a(z)$ and $V_b(z)$ are potentials of the plates a and b, respectively. The subscript "0" marks the values at the inlet ($z = 0$).

V_{ab} is equal to the voltage of cell A V_{cell} (Fig. 2). The latter is given by

$$V_{cell} = V_{oc} - \eta^a(z) - \eta^c(z) - R_c(z)j(z) \qquad [2]$$

Here V_{oc} is cell open-circuit voltage, η^a and η^c are polarization voltages of the anode and the cathode sides, respectively, R_c is local contact resistance, and j is local current density in cell A. The superscripts a and c refer to the anode and the cathode sides, respectively.

Equating Eq. 2 and 1, we find

$$\eta^a(z) + \eta^c(z) = E_0 - [V_a(z) - V_b(z)] - R_c j(z) \qquad [3]$$

where

$$E_0 = V_{oc} - V_0 \qquad [4]$$

is voltage loss in the cell at $z = 0$.

It is convenient to introduce dimensionless variables

$$\widetilde{\eta} = \frac{\eta}{b^a}, \quad \widetilde{V} = \frac{V}{b^a}, \quad \widetilde{E} = \frac{E}{b^a}, \quad \widetilde{j} = \frac{j}{j^a_{\lim}}, \quad \widetilde{R} = \frac{Rj^a_{\lim}}{b^a},$$
$$\widetilde{\psi} = \frac{\psi}{\psi_0}, \quad \widetilde{\xi} = \frac{\xi}{\xi_0} \qquad [5]$$

Here b^a is Tafel slope on the anode side, $j^a_{\lim} = 6FD^a c^a \psi_0 / l^a$ is the limiting current density due to methanol transport through the anode backing layer, D^a is methanol diffusion coefficient in the backing layer of a thickness l^a, c^a is the total molar concentration in the anode channel, ξ and ψ are oxygen and methanol molar fractions in the respective channel, and ξ_0 and ψ_0 are their inlet values.

Using explicit expressions for $\widetilde{\eta}^a$ and $\widetilde{\eta}^{c12}$ in Eq. 3, we get

$$\ln\left(\frac{\widetilde{j}}{q\widetilde{\psi}}\right) - \ln\left(1 - \frac{\widetilde{j}}{\widetilde{\psi}}\right) + \ln(1+\beta) + p\left[\ln\left(\frac{\widetilde{j}}{\alpha q\widetilde{\xi}}\right) - \ln\left(1 - \frac{\widetilde{j} + \beta_*(\widetilde{\psi} - \widetilde{j})}{\gamma\widetilde{\xi}}\right)\right] = \widetilde{E}_0 - (\widetilde{V}_a - \widetilde{V}_b) - \widetilde{R}_c\widetilde{j} \qquad [6]$$

Here $p = b^c/b^a$ is the ratio of Tafel slopes on the cathode and the anode sides, $\beta_* = \beta/(1+\beta)$, $\beta = D_m l^a/(D^a l_m)$ describes the rate of methanol crossover through the membrane, and D_m is methanol diffusion coefficient in membrane of a thickness l_m. Qualitatively, the larger crossover, the larger β and β_* (note that $0 \le \beta_* \le 1$).

Parameters q, α, and γ are

$$q = \frac{l^a_t i^a_* l^a}{6FD^a c^a_{\text{ref}}}, \quad \alpha = \frac{l^c_t i^c_* c^a_{\text{ref}}}{l^a_t i^a_* c^c_{\text{ref}}}\left(\frac{c^c\xi^0}{c^a\psi^0}\right), \quad \gamma = \frac{2D^c l^a}{3D^a l^c}\left(\frac{c^c\xi^0}{c^a\psi^0}\right) \qquad [7]$$

Here l_t is the thickness of the catalyst layer, i_* is the volumetric exchange current density (A cm^{-3}), D^c is the oxygen diffusion coefficient in the backing layer of the thickness l^c, c^a_{ref} and c^c_{ref} are reference molar concentrations of methanol and oxygen, respectively, and c is total molar concentration in the channel.

The left side of Eq. 6 contains voltage losses on both sides of the cell due to activation of electrochemical reactions, transport of reactants through the respective backing layer, and methanol crossover through the membrane (the terms with β and β_*). For the detailed discussion of the terms on the left side of Eq. 6, please see Ref. 11 and 12.

Effective cell potential and voltage loss in the cell.— Equation 2 shows that cell voltage depends on z. The external circuit, however, "feels" a single value of effective cell voltage V_{eff}, which is a function of current in the stack only. Evidently, the sum over all cells $\Sigma V_{\text{eff}} = V_{\text{stack}}$, where V_{stack} is the stack voltage.

V_{eff} results from the following arguments. Using Eq. 4 we can rewrite Eq. 2 as

$$V_{\text{cell}}(z) = V_{\text{oc}} - E_0 + [V_a(z) - V_b(z)] \qquad [8]$$

Multiplying Eq. 8 by $wj(z)$ and integrating the result over z, we get total electric power generated in cell A

$$P = w\int_0^L V_{\text{cell}} j dz = wLJ(V_{\text{oc}} - E_0) + w\int_0^L (V_a - V_b) j dz \qquad [9]$$

where

$$J = \frac{1}{L}\int_0^L j dz \qquad [10]$$

is the mean current density in the cell.

Clearly, V_{eff} is the voltage, which provides the same value of P

$$wLJV_{\text{eff}} = P \qquad [11]$$

It is convenient to introduce the total voltage loss in the cell U according to

$$V_{\text{eff}} = V_{\text{oc}} - U \qquad [12]$$

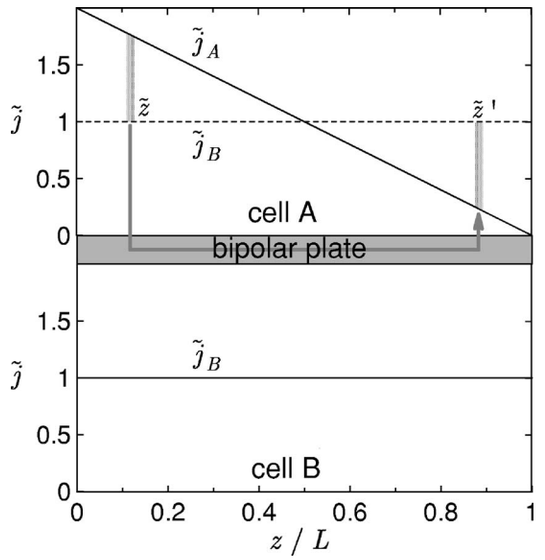

Figure 3. To the transport of current along the bipolar plate. Local current $\tilde{j}_A$ in cell A linearly decreases with z and in cell B local current $\tilde{j}_B$ is constant. To fulfill local balance of currents the difference $(\tilde{j}_A - \tilde{j}_B)d\tilde{z}$ (dotted area) has to be transported from $\tilde{z}$ to $\tilde{z}'$ along the bipolar plate.

Equating Eq. 9 and 11, and taking into account Eq. 12, we get

$$U = E_0 + \frac{1}{LJ}\int_0^L (V_a - V_b)jdz \qquad [13]$$

In dimensionless variables Eq. 13 reads

$$\tilde{U} = \tilde{E}_0 + \frac{1}{\tilde{J}}\int_0^1 (\tilde{V}_a - \tilde{V}_b)\tilde{j}d\tilde{z} \qquad [14]$$

To characterize the stack we use the average voltage loss per cell in the stack $\tilde{U}_{\text{av}} = (\Sigma_i \tilde{U}_i)/N_{\text{cell}}$. Here summation is performed over all cells and N_{cell} is the number of cells in the stack.

Local potential of the plate.— The right side of Eq. 6 contains local voltage drop $\tilde{V}_a - \tilde{V}_b$ between two BPs, which clamp cell A (Fig. 2). Potential of BP obeys the Poisson equation.[5] In the dimensionless variables Eq. 5, the equation for plate a reads

$$\frac{\partial^2 \tilde{V}_a}{\partial \tilde{z}^2} = \tilde{R}(\tilde{j}_C - \tilde{j}) \qquad [15]$$

where $\tilde{j}_C$ is local current in cell C (Fig. 2) and $\tilde{R}$ is dimensionless resistivity of BP.[a]

Physically, each BP transports along z the difference of local currents in the adjacent cells. BP serves as an equalizer; it redistributes along z the excess of local current generated in cell A in order to transport this current through cell B (Fig. 3). Formal analysis[5] leads to Eq. 15.

Quite analogous, for plate b we write

$$\frac{\partial^2 \tilde{V}_b}{\partial \tilde{z}^2} = \tilde{R}(\tilde{j} - \tilde{j}_B) \qquad [16]$$

where $\tilde{j}_B$ is local current density in cell B.

[a] R_a (Ω cm^2) is expressed through the conductivity of BP material σ as $R = L^2/\sigma h$, where h is BP thickness.

Mass conservation equations.— Polarization voltages of the anode and the cathode sides in Eq. 6 depend on methanol and oxygen molar fraction in the anode and the cathode channel, respectively. These fractions obey the mass conservation equations[12]

$$\lambda^a \tilde{J}\frac{\partial \tilde{\psi}}{\partial \tilde{z}} = -[\tilde{j} + \beta_*(\tilde{\psi} - \tilde{j})], \quad \tilde{\psi}(0) = 1 \qquad [17]$$

$$\lambda^c \tilde{J}\frac{\partial \tilde{\xi}}{\partial \tilde{z}} = -[\tilde{j} + \beta_*(\tilde{\psi} - \tilde{j})], \quad \tilde{\xi}(0) = 1 \qquad [18]$$

Here λ^a and λ^c are stoichiometry of methanol and oxygen flows, respectively, and $\tilde{J} = \int_0^1 \tilde{j}d\tilde{z}$ is dimensionless mean current density in a cell.

The right sides of Eq. 17 and 18 describe consumption of feed molecules in the useful reactions (the term $-\tilde{j}$) and in the direct "burning" on the cathode side due to methanol crossover (the terms with β_*). For a detailed discussion of Eq. 17 and 18, please see Ref. 12 and 13.

Equation for local current.— It is convenient to transform Eq. 6 into a differential equation for $\tilde{j}$. Differentiating Eq. 6 with respect to $\tilde{z}$ and using Eq. 17 and 18 to exclude derivatives $\partial\tilde{\psi}/\partial\tilde{z}$ and $\partial\tilde{\xi}/\partial\tilde{z}$, respectively, we get

$$\frac{\partial \tilde{j}}{\partial \tilde{z}} = \frac{N_j}{D_j}, \quad \tilde{j}(0) = \tilde{j}_0 \qquad [19]$$

where

$$N_j = \lambda^a\lambda^c\tilde{J}(1+\beta)(\tilde{\psi} - \tilde{j})\tilde{j}[\beta\tilde{\psi} + \tilde{j} - \gamma(1+\beta)\tilde{\xi}]\left[\tilde{j}\frac{\partial \tilde{R}_c}{\partial \tilde{z}} + \frac{\partial (\tilde{V}_a - \tilde{V}_b)}{\partial \tilde{z}}\right] - \tilde{j}(\tilde{j} + \beta\tilde{\psi})[p\lambda^a\gamma(1+\beta)(\tilde{\psi} - \tilde{j}) - \lambda^c\beta(1+p)\tilde{\psi} + \beta\lambda^c(p\tilde{j} + \gamma\tilde{\xi}) + \lambda^c(\gamma\tilde{\xi} - \tilde{j})] \qquad [20]$$

and

$$D_j = -\lambda^a\lambda^c\tilde{J}(1+\beta)(\tilde{\psi} - \tilde{j})\tilde{j}[\beta\tilde{\psi} + \tilde{j} - \gamma(1+\beta)\tilde{\xi}]\tilde{R}_c + \lambda^a\lambda^c\tilde{J}(1+\beta)\{\gamma\beta(\tilde{\psi} - p\tilde{j})\tilde{\xi} + p(\beta\tilde{\psi} - \gamma\tilde{\xi})\tilde{j} + \gamma[1 + p(1+\beta)]\tilde{\psi}\tilde{\xi} - \tilde{\psi}\tilde{j} - (1+p)\beta\tilde{\psi}^2\} \qquad [21]$$

Initial condition $\tilde{j}_0$ for Eq. 19 is a solution to the equation

$$\ln\left(\frac{\tilde{j}_0}{q}\right) - \ln(1 - \tilde{j}_0) + \ln(1+\beta) + p\left\{\ln\left(\frac{\tilde{j}_0}{\alpha q}\right) - \ln\left[1 - \frac{\tilde{j}_0 + \beta_*(1 - \tilde{j}_0)}{\gamma}\right]\right\} = \tilde{E}_0 - \tilde{R}_c(0)\tilde{j}_0 \qquad [22]$$

which is Eq. 6 with $\tilde{z} = 0$, $\tilde{\psi} = \tilde{\xi} = 1$, and $\tilde{V}_a = \tilde{V}_b = 0$.

Stack Model

Equations 17-19 with $\tilde{V}_a$ and $\tilde{V}_b$ given by Eq. 15 and 16, respectively, describe the performance of an individual cell clamped between two BPs with the finite conductivity. Using these equations we can assemble a stack model as follows.

Consider two adjacent cells A and B in the stack (Fig. 2). Local potential of cell A is equal to the difference of local potentials of bipolar plates a and b. According to Eq. 15 and 16, these potentials are in turn determined by the local current densities in the adjacent cells (Fig. 2). For the stack we thus have a selfconsistent problem, which has to be solved iteratively:

Table I. Parameters for the simulation.

Number of cells in the stack	100
Methanol stoichiometry	2
Oxygen stoichiometry	2
Conductivity of the bipolar plate (Ω^{-1} cm^{-1})	200
Bipolar plate length (cm)	10
Bipolar plate thickness (cm)	0.1
Bipolar plate resistivity (Ω cm^2)	5
Characteristic size of the spot Δ in Eq. 23 (dimensionless)	0.02
Tafel slope of the anode side b^a (V)	0.05
Limiting current density j^a_{lim} (A cm^{-2})	1
Dimensionless resistivity of BP $\widetilde{R}$	100
Parameters in Eq. 6, 19, and 22:	
α	20.038
β	1.0
γ	2.805
p	1.0
q	1.727×10^{-5}

1. Assuming that all BPs are ideally conductive ($\widetilde{V}_a = \widetilde{V}_b = 0$), solve the system 17-19 for all cells in a stack.
2. Using new local current in the cells, solve Eq. 15 for all bipolar plates.
3. With the new $\widetilde{V}_a(\widetilde{z})$, $\widetilde{V}_b(\widetilde{z})$ solve the system 17-19 for each cell in a stack.
4. Repeat steps 2 and 3 until convergence is achieved.

Because each cell transports current only between neighbors (e.g., cell A transports current from B to C), the code can be effectively parallelized. The solution of Eq. 17-19 (step 3) for each cell (or for a block of the cells) can be performed on a separate processor. Before execution of step 2 the cells (blocks) exchange information with the neighbors.

Results and Discussion

The results below are presented for the 100 cell stack. The cell and operational parameters are listed in Table I. The physical parameters, which appear in Eq. 7 are listed in Table II.

Local resistive spots are assumed to have Gaussian shape

$$R_c = R_c^0 \exp\left(-\frac{(\widetilde{z} - \widetilde{z}_0)^2}{\Delta^2}\right) \qquad [23]$$

To study the effect of multiple spots on stack performance, we performed a series of calculations, varying the number of randomly positioned spots in each cell. Figure 4 illustrates the variant with the two spots in every cell.

Table II. Parameters of the individual cells.

Diffusion coefficient of methanol in the backing layer (cm^2 s^{-1})	1×10^{-5}
Diffusion coefficient of methanol in the membrane (cm^2 s^{-1})	1×10^{-5}
Oxygen diffusion coefficient in the cathode backing layer (cm^2 s^{-1})	3×10^{-3}
Exchange current density on the cathode side (A cm^{-3})	10^{-2}
Exchange current density on the anode side (A cm^{-3})	1
Thickness of the backing layer (anode and cathode, cm)	0.01
Membrane thickness (cm)	0.01
Catalyst layer thickness (anode and cathode, cm)	0.001
Oxygen molar fraction at the inlet	0.21
Oxygen pressure at the inlet (bara)	2
Methanol molar concentration at the inlet (M)	1
Cell temperature (C)	70

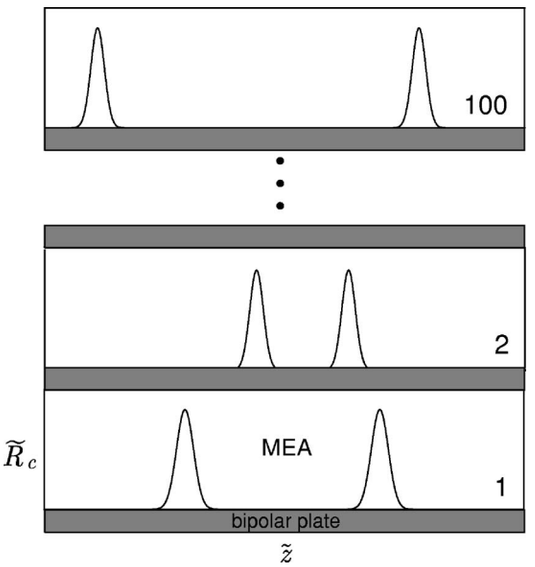

Figure 4. Sketch of 100 cell DMFC stack. Each cell has two randomly positioned local spots of high contact resistance.

Figure 5 shows stack polarization curves (average voltage loss per cell vs mean current density) when each cell has indicated number of spots. The main effect is clearly seen: the spots reduce stack limiting current density. The more spots in each cell the lower the limiting current density (Fig. 5). The reduction of limiting current is accompanied by the decrease in the curvature of the polarization curve (Fig. 5), which indicates high resistive losses.

The origin of limiting current reduction is clear from Fig. 6, which shows the z–shapes of local current density and polarization voltages of the anode and the cathode sides in the middle of the stack (in the 50th cell). Potential of the bipolar plate separating the 49th and 50th cell is also shown. Each cell has 4 spots and total current in the stack is close to the limiting one (the respective point on polarization curve is indicated by the bold dot in Fig. 5). For comparison the curves for the stack without the spots are also depicted.

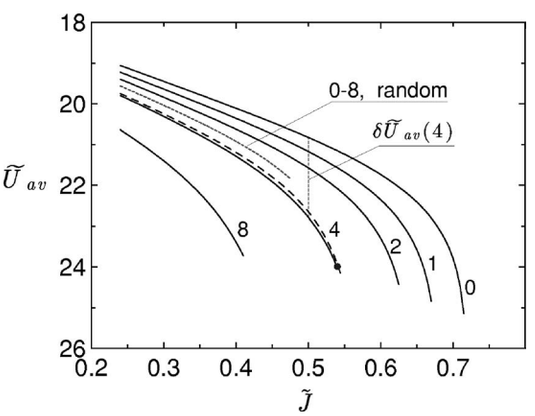

Figure 5. Stack polarization curves for indicated number of spots in each cell. Shown is average (per cell) voltage loss in the stack $\widetilde{U}_{\text{av}}$ vs mean current density $\widetilde{J}$. All variables are dimensionless. Plate resistivity $\widetilde{R} = 100$ (Table I). (short–dashed curve) Random number (in the range 0–8) of spots in each cell. (long–dashed curve) 4 spots per cell, $\widetilde{R} = 10$. $\delta\widetilde{U}_{av}(4)$, the average voltage loss due to 4 spots in each cell is the difference of the curves for 0 and 4 spots.

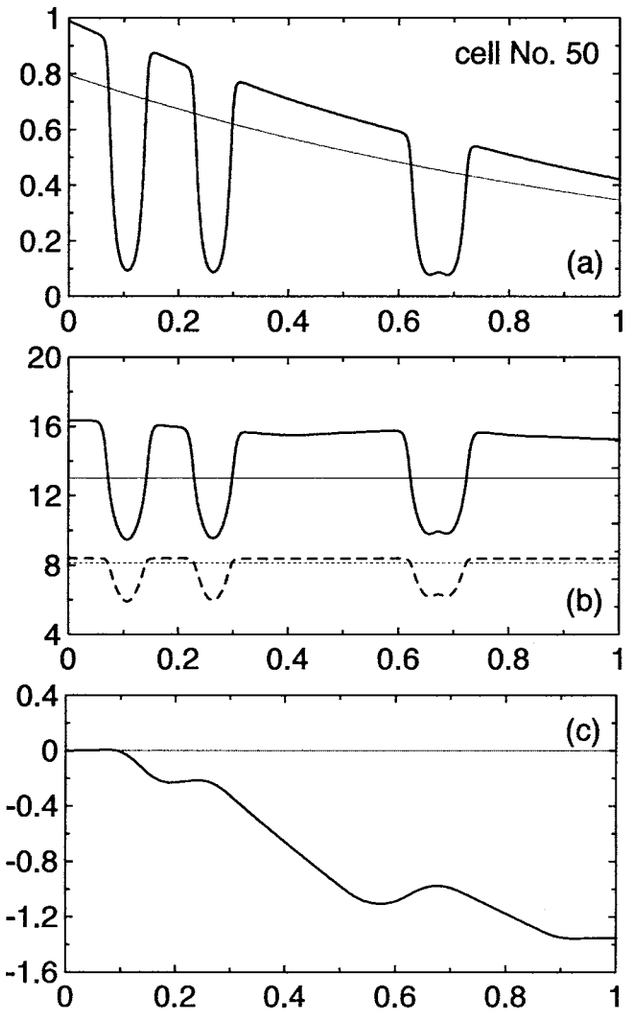

Figure 6. (a) Local current density, (b) the anode and the cathode polarization voltages in the middle of the stack (cell no. 50) and (c) potential of the bipolar plate between 49th and 50th cells. (thin lines) no spots and (thick lines) 4 spots in each cell. Solid curves in (b) show polarization voltage of the anode side, dashed curves of the cathode side.

Each spot locally blocks the generation of current in a cell; the missing current has to be produced in the unaffected part of the cell. Therefore, the anode and the cathode polarization voltages in the unaffected part of the cell increase (Fig. 6).[b]

In other words, the spots increase the polarization loss in a stack. This is the main effect of spots: in the studied range of parameters (n = 1–8, $\widetilde{R}_c$ = 100, and σ = 0.02) the average voltage loss due to $\delta\widetilde{U}_{\rm av}(n) \equiv \widetilde{U}_{\rm av}(n) - \widetilde{U}_{\rm av}(0)$ dominates the direct loss caused by the transport of current along the bipolar plate $\widetilde{V}_{bp} = (\Sigma_i \widetilde{V}_i^{\rm loss})/N_{\rm cell}$.[c] Here $\widetilde{U}_{\rm av}(n)$ is the average (per cell) voltage loss for the case of n spots in each cell (Fig. 5).

$\delta\widetilde{U}_{\rm av}(n)$ and $\widetilde{V}_{bp}$ are shown in Fig. 7. It is seen that $\widetilde{V}_{bp}$ is much less than $\delta\widetilde{U}_{\rm av}(n)$. This result is also illustrated in Fig. 5, where the long–dashed curve exhibits performance of the stack with 4 spots

[b]Note that $\widetilde{\eta}^a$ grows larger because exchange current density on the anode side is taken to be lower, than on the cathode side (Table I).

[c]The calculation of $\widetilde{V}_i^{\rm loss}$ is described in the Appendix.

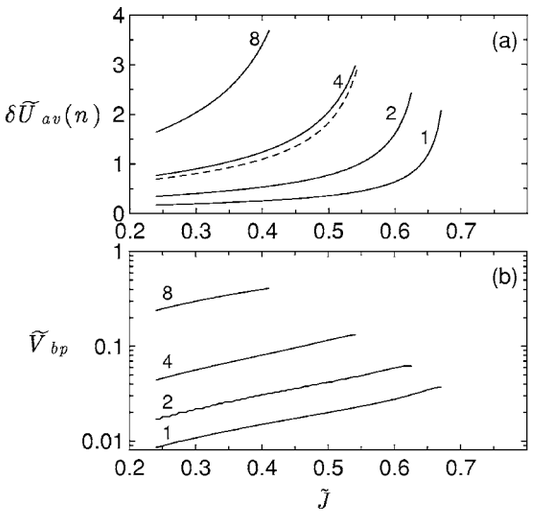

Figure 7. Voltage losses vs mean current density in the stack for the indicated number of spots in each cell. (a) Average (per cell) total voltage loss $\delta\widetilde{U}_{av}(n)$ due to n spots in each cell. The meaning of $\delta\widetilde{U}_{av}(n)$ is illustrated in Fig. 5. (b) Average (per cell) voltage loss $\widetilde{V}_{bp}$ due to in–plane current in the bipolar plates.

per cell and 10 times lower resistivity of BP ($\widetilde{R}$ = 10). This curve practically coincides with the curve for n = 4 and $\widetilde{R}$ = 100.

Conclusions

A model of a DMFC stack is developed. The model is based on our recent model of a single cell, which takes into account transport of reactants across the cell (including methanol crossover) and their transport along the channel. Kinetics of electrochemical reactions on both sides of the cell is assumed to obey the Tafel law.

The stack model accounts for in–plane current in the bipolar plates and voltage loss due to the "spots" of local resistance. It is shown that the effect of spots is twofold. They (*i*) increase polarization losses in the contaminated cells and (*ii*) induce in–plane currents in the bipolar plates. In the studied range of parameters the main effect of spots is the growth of polarization losses.

Research Center Juelich assisted in meeting the publication costs of this article.

APPENDIX

To calculate voltage loss due to in–plane current in the bipolar plate a we replace the plate with the equivalent resistance, which dissipates the same electric power and supports mean current in the stack. Thus, voltage loss on the equivalent resistance is

$$V_a^{\rm loss} = \frac{P_a}{LwJ} \qquad [A\text{-}1]$$

where P_a is total power dissipated in the plate.

Local in-plane current in the plate a is[5] (Fig. 2)

$$I(z) = w\int_0^z (j_C - j)dz \qquad [A\text{-}2]$$

Local voltage loss on the interval δz due to current I is

$$\delta V_a = I(z)r\delta z \qquad [A\text{-}3]$$

where r is linear resistivity of the plate (Ω cm^{-1}). Total electric power dissipated in the plate is

$$P_a = \int_0^L I(z)\frac{\partial V_a}{\partial z}dz = r\int_0^L I^2 dz = rw^2\int_0^L \left[\int_0^z (j_C - j)ds\right]^2 dz \qquad [A\text{-}4]$$

Using Eq. A-4 and A-2 in A-1 we finally obtain

$$V_a^{\text{loss}} = \frac{rw}{LJ}\int_0^L \left(\int_0^z (j_C - j)ds\right)^2 dz$$

Note that

$$R = \frac{L^2}{\sigma h} = L^2 rw$$

List of Symbols

$\sim$	marks dimensionless variables
b	Tafel slope, V
c	total molar concentration in the channel, mol cm^{-3}
c_{ref}	reference molar concentration, mol cm^{-3}
D^a	methanol diffusion coefficient in the backing layer, cm^2 s^{-1}
D^c	oxygen diffusion coefficient in the backing layer, cm^2 s^{-1}
D_m	methanol diffusion coefficient in the membrane, cm^2 s^{-1}
E_0	total voltage loss at $z = 0$, V
F	Faraday constant, 9.6495×10^4 Coulomb mol^{-1}
i_*	exchange current density per unit volume, A cm^{-3}
J	mean current density in a cell, A cm^{-2}
j	local current density in a cell, A cm^{-2}
j_{lim}	limiting current density, A cm^{-2}
h	thickness of bipolar plate, cm
l	thickness of the backing layer, cm
l_m	thickness of the membrane, cm
l_t	thickness of the catalyst layer, cm
L	length of the current collector plate/channel, cm
N_{cell}	number of cells in the stack
P	electric power, W
p	ratio of Tafel slopes, $p = b^c/b^a$
q	dimensionless parameter, 7
R	resistivity of bipolar plate, Ω cm^2
R_c	contact resistance, Ω cm^2
U	total voltage loss in a cell, V
$\delta U_{av}(n)$	average voltage loss (per cell) due to n spots in each cell to the total voltage loss in the stack, V
V_a	potential of the bipolar plate a, V
V_{bp}	average (per cell) voltage loss due to in–plane current in the bipolar plate, V
V_{cell}	local cell voltage, V
V_{oc}	thermodynamic open-circuit voltage, V
V_0	local potential between two bipolar plates at $z = 0$, V
w	width of the bipolar plate, cm
x	coordinate in the through–plane direction, cm
z	coordinate along the channel, cm

Greek

α	dimensionless parameter, 7
β	dimensionless parameter
β_*	$\beta_* = \beta/(1 + \beta)$
Δ	characteristic gaussian width of a spot, cm
γ	dimensionless parameter, 7
η	polarization voltage, V
σ	conductivity of the bipolar plate, Ω^{-1} cm^{-1}
λ	stoichiometry of feed flow
ξ	oxygen molar fraction in the cathode channel
ψ	methanol molar fraction in the anode channel

Superscripts

a	anode side
c	cathode side

Subscripts

0	inlet (at $\tilde{z} = z = 0$)
a	bipolar plate a
b	bipolar plate b
bp	any bipolar plate
lim	limiting

References

1. A. S. Aricò, S. Srinivasan, and V. Antonucci, *Fuel Cells*, **1**, 133 (2001).
2. H. Yang, T. S. Zhao, and Q. Ye, *J. Power Sources*, **139**, 79 (2005).
3. A. A. Kulikovsky, *Electrochem. Commun.* **7**, 237 (2005).
4. A. A. Kulikovsky, *Electrochim. Acta*, **51**, 2003 (2006).
5. A. A. Kulikovsky, *J. Power Sources*, doi: 10.1016/j.jpowsour.2006.01.058
6. D. Buttin, M. Dupont, M. Straumann, R. Gille, J.-C. Dubois, R. Ornealas, G. P. Fleba, E. Ramunni, V. Antonucci, A. S. Aricò, P. Creti, E. Modica, P. Pham-Thi, and J.-P. Ganne, *J. Appl. Electrochem.*, **31**, 275 (2001).
7. E. Birgersson, J. Nordlund, H. Ekström, M. Vynnycky, and G. Lindbergh, *J. Electrochem. Soc.*, **150** A1368 (2003).
8. E. Birgersson, J. Nordlund, M. Vynnycky, C. Picard, and G. Lindbergh, *J. Electrochem. Soc.*, **151**, A2157 (2004).
9. J. Divisek, J. Fuhrmann, K. Gärtner, and R. Jung, *J. Electrochem. Soc.*, **150**, A811 (2003).
10. B. L. Garcia, V. A. Sethuraman, J. W. Weidner, R. E. White, and R. Dougal, *J. Fuel Cell Sci. Technol.*, **1**, 43 (2004).
11. A. A. Kulikovsky, *Electrochem. Commun.*, **4**, 939 (2002).
12. A. A. Kulikovsky, *J. Electrochem. Soc.*, **152**, A1121 (2005).
13. A. A. Kulikovsky, *Electrochem. Commun.*, **6**, 1259 (2004).